

## **Creep damage by multiple cavity growth controlled by grain boundary diffusion**

Bernard Fedelich<sup>1</sup>, Jack Owen<sup>2</sup>

<sup>1</sup>*Bundesanstalt für Materialforschung und -prüfung, (BAM), Berlin, Germany*

<sup>2</sup>*Ecole Nationale des Ponts et Chaussées, (ENPC), Marne la Vallée, France*

**Abstract:** A novel procedure to solve the diffusion problem on a cavitated grain boundary has been developed. Cavities are assumed to maintain their quasi-equilibrium form. The solution relies on a representation of the local normal stress by holomorphic complex functions on the grain boundary plane. The cavity volume growth rates are calculated and the solution is used to simulate the cavitation process, taking into account cavity nucleation, growth, sintering and coalescence. The results are compared with the classical homogeneous solution, which assumes a uniform cavity size and spacing. It is found that the classical solution strongly overestimates the kinetics of the porosity evolution.

### **1. Introduction**

Most models of creep porosity implicitly assume a uniformly distributed array of equally sized voids on a grain boundary. These models can be seen as further improvements of the axisymmetric solution for one void, initially proposed by Hull and Rimmer [1], to include the effects of cavity surface diffusion or plastic creep flow. A review of these developments can be found, e.g. in [2].

In parallel, it has been early recognized that the normal stress acting on a damaged grain boundary can be considerably reduced by the stress redistribution induced by the separation of the grains adjacent to the damaged grain boundary (constrained cavity growth). The analysis of this effect, which is essential for the failure time prediction, requires an estimate of the kinetics of grain separation (grain boundary thickening) and a structural analysis of the stress redistribution. The solution proposed by Rice [3] is based on simplified analytic solutions for cracked bodies. A much more sophisticated approach was proposed in a series of papers by Van der Giessen and co-workers [4] and [5], which is based on a cohesive model of the grain boundary. Note that all these models heavily rely on the axisymmetric solution, i.e. on a uniform void distribution.

However, a non uniform distribution of voids on a grain boundary decreases the void growth rate with respect to the uniform distribution. This has been clearly demonstrated for one-dimensional random arrays of cavities [6,7] and for two dimensional random arrangements of cavities [8]. With an approximate solution it was shown [9] that void clustering tends to reduce the average growth rate.

Cavities are usually continually nucleated, with a birth rate that correlates with the creep strain rate [10] or grain boundary sliding [11]. Simulations of void nucleation, growth and coalescence with one-dimensional arrays [12,13] demonstrated that nucleation is the most dominant factor determining rupture time, while differences in the cavity growth mode only play minor roles. Void coalescence and sintering also contribute to reduce the damage rate on the grain

boundary. The more realistic case of a two dimensional distribution is much more challenging due to the complicated interactions between the cavities. Under the assumption of a uniform void size and simplified interactions a statistic theory of the cavitation process (nucleation, growth, sintering and coalescence) has been proposed in [14,15].

Finally, the relationship between the fraction  $\omega$  of the cavitated grain boundary and the degree of grain boundary thickening not only depends on the average void size but on the whole void size distribution. Cavitation simulations of a one-dimensional array [16] show that the uniform cavity size and spacing assumptions considerably overestimate the grain separation rate. Thus, a reliable analysis of the stress redistribution due to the separation of the grains requires keeping track of the cavity size distribution.

This work presents an original numerical solution to the grain boundary diffusion problem in the case of quasi-equilibrium cavities (fast surface diffusion). This solution is then applied to simulate the cavitation of a representative grain boundary element (RGE), including the effects of void nucleation, growth, coalescence and sintering. The RGE is analogous to the usual concept of representative volume element in the mechanics of heterogeneous materials.

The results can be used to identify a law relating the local stress on the boundary and the separation rate of the adjacent grains for application in cohesive zone models. The cohesive zone model can then be embedded in a Finite Element model of a polycrystal [4,5] to accurately assess the locally acting stresses.

## 2. System equations

The following analysis focuses on a circular RGE  $S_0$  of radius  $R$ , weakened by  $N$  cavities having the shape of spherical caps with radius  $a_i$  and centred at  $\mathbf{c}_i$ ,  $1 \leq i \leq N$  (Fig.1). The cavitated part of  $S_0$  is denoted  $S_d$  and the intact part of the RGE is  $S = S_0 - S_d$ . The void surface makes an angle  $\psi = \cos^{-1} \left( \frac{\gamma_{gb}}{2\gamma_s} \right)$  with the grain boundary, where  $\gamma_s$  is the specific surface energy of a free surface and  $\gamma_{gb}$  the surface energy of the grain boundary. The corresponding volume of an individual cavity  $i$  is given by

$$V_i = \frac{4}{3} \pi h(\psi) a_i^3, \quad \text{where } h(\psi) = \left[ (1 + \cos \psi)^{-1} - \frac{1}{2} \cos \psi \right] / \sin \psi. \quad (1)$$

If  $\sigma$  is the local normal stress and  $\llbracket \dot{u}^p \rrbracket$  the rate of separation of the adjacent grains, the conservation equation (see [2]) leads to

$$\Delta \sigma + \frac{1}{D} \llbracket \dot{u}^p \rrbracket = 0 \quad \text{in } S, \quad (2)$$

where  $D = \frac{\Omega \delta D_{gb}}{k T} = \frac{\Omega \delta D_{gb0}}{k T} \exp \left( -\frac{Q_b}{RT} \right)$  ( $\delta D_{gb}$  = grain boundary diffusion coefficient,  $\Omega$  = atomic volume,  $kT$  = energy per atom measure of temperature) with the boundary condition at the tip  $L_i$  of the cavities

$$\sigma = \sigma_i = \frac{2 \sin \psi \gamma_s}{a_i} \quad \text{on } L_i. \quad (3)$$

With these notations, the diffusive flux of atoms in the grain boundary is

$$\mathbf{j} = \frac{\delta D_{gb}}{kT} \nabla \sigma. \quad (4)$$

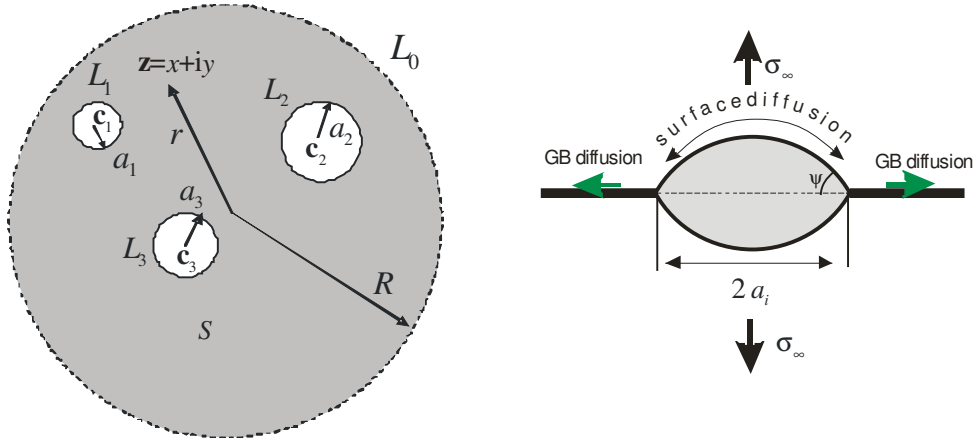


Fig. 1. Notations of the representative grain boundary element (RGBE).

On the boundary  $L_0$  of the RGBE, we assume local symmetry, i.e. the flux  $\mathbf{j} \cdot \mathbf{n}$  of atoms is assumed to vanish, or equivalently

$$\frac{\partial \sigma}{\partial r} = 0 \quad \text{on } L_0. \quad (5)$$

If a global normal stress  $\sigma_\infty$  acts on the grain boundary, the equilibrium requires

$$\iint_S \sigma dS = S_0 \sigma_\infty = \pi R^2 \sigma_\infty. \quad (6)$$

Finally, the rate of volume growth  $\dot{V}_i$  of an individual cavity is the sum of the contributions of the atoms diffusive flux on its boundary and grain boundary thickening

$$\dot{V}_i = \Omega \oint_{L_i} \mathbf{j} \cdot \mathbf{n} ds + \pi a_i^2 \left[ \left[ \dot{u}^p \right] \right]. \quad (7)$$

### 3. Resolution procedure

The system constituted of the equations (2), (3), (5) and (6) is solved in the complex plane  $\mathbf{z} = x + iy$ . The particular solution  $\sigma_0 = -\frac{\left[ \left[ \dot{u}^p \right] \right]}{4\mathcal{D}} r^2$  of eq. (2) is introduced and the new unknown function  $\sigma_h = \sigma - \sigma_0$ , which is harmonic in the multiply connected region  $S$ , satisfies the system

$$\begin{aligned}
 \Delta\sigma_h &= 0 \quad \text{in } S, \\
 \sigma_h &= \sigma_i - \sigma_0 \quad \text{on } L_i, \\
 \frac{\partial\sigma_h}{\partial r} &= -\frac{\partial\sigma_0}{\partial r} = \frac{\llbracket \dot{u}^p \rrbracket}{2\mathcal{D}} R \quad \text{on } L_0, \\
 \iint_S \sigma_h dS &= \pi R^2 \sigma_\infty - \iint_S \sigma_0 dS.
 \end{aligned} \tag{8}$$

A classical result of the theory of complex functions [17] states that  $\sigma_h$  can be represented with the real part of some holomorphic function  $\mathbf{f}(\mathbf{z})$  in  $S$

$$\sigma_h(\mathbf{z}) = \text{Re}(\mathbf{f}(\mathbf{z})) + \sum_{k=1}^N \Lambda_k \ln \frac{|\mathbf{z} - \mathbf{c}_k|}{R}, \tag{9}$$

where  $\Lambda_k$  are  $N$  real numbers. Using a generalization of the theorem of Laurent to a  $N$  times multiply connected region [18], the holomorphic function  $\mathbf{f}(\mathbf{z})$  has an explicit representation of the form

$$\mathbf{f}(\mathbf{z}) = \mathbf{Z}_{0,0} + \sum_{m=1}^{+\infty} \mathbf{Z}_{0,m} \left( \frac{\mathbf{z}}{R} \right)^m + \sum_{k=1}^N \sum_{m=1}^{+\infty} \mathbf{Z}_{k,m} \left( \frac{\mathbf{z} - \mathbf{c}_k}{a_k} \right)^{-m}, \tag{10}$$

where  $\mathbf{Z}_{0,0}$  and  $\mathbf{Z}_{k,m} = X_{k,m} + iY_{k,m}$ ,  $0 \leq k \leq N$ ,  $1 \leq m \leq \infty$ , are complex numbers. The function  $\sigma_h(\mathbf{z})$  defined in  $S$  by eq. (9) and (10) is harmonic. It can also readily be shown that the volume growth rate (7) of a cavity  $i$  is

$$\dot{V}_i = 2\pi \mathcal{D} \Lambda_i. \tag{11}$$

The unknown real values  $\llbracket \dot{u}^p \rrbracket, \Lambda_k, X_{0,0}, X_{0,m}, Y_{0,m}, X_{k,m}, Y_{k,m}$  with  $1 \leq k \leq N$ ,  $1 \leq m \leq \infty$  have to be determined from the boundary conditions (8)<sub>2</sub> and (8)<sub>3</sub> and the equilibrium of forces (8)<sub>4</sub>. In practice, the infinite series in (10) are truncated. We used the same order of truncation  $m \leq M$  for both series types, i.e.

$$\sigma_h(\mathbf{z}) \approx X_{0,0} + \text{Re} \left[ \sum_{m=1}^M \mathbf{Z}_{0,m} \left( \frac{\mathbf{z}}{R} \right)^m + \sum_{k=1}^N \sum_{m=1}^M \mathbf{Z}_{k,m} \left( \frac{\mathbf{z} - \mathbf{c}_k}{a_k} \right)^{-m} \right] + \sum_{k=1}^N \Lambda_k \ln \frac{|\mathbf{z} - \mathbf{c}_k|}{R}. \tag{12}$$

The total number of real unknowns is  $1 + (2M + 1)(N + 1)$ . Formally, the conditions (8)<sub>2</sub> to (8)<sub>4</sub> have the general form

$$F_k(\theta; \Lambda_k, X_{0,0}, X_{0,m}, Y_{0,m}, X_{k,m}, Y_{k,m}) = G_k(\theta; \llbracket \dot{u}^p \rrbracket), \quad \forall \theta, 0 \leq \theta \leq 2\pi \tag{13}$$

on the  $1 + N$  circles  $L_0, L_k, 1 \leq k \leq N$ . The equations (13) have been solved in the Fourier space. If the Fourier series are truncated at the same order  $P$  we obtain all in all  $(N + 1)(2P + 1) + 1$  equations (taking also the equilibrium equation into account) for the coefficients. By setting  $P = M$  we just have as many equations as necessary.

To simplify the evaluation of the equilibrium condition, the surface integral in (8)<sub>4</sub> can also be transformed into integrals on the circles  $L_k$ , by using the fact that  $\sigma_h$  is harmonic, i.e.

$$\iint_S \sigma_h dS = \frac{1}{4} \oint_{\partial S} \frac{\partial r^2}{\partial n} \sigma_h dl - \frac{1}{4} \oint_{\partial S} r^2 \frac{\partial \sigma_h}{\partial n} dl, \tag{14}$$

where  $\partial S = \bigcup_{k=0}^N L_k$  is the boundary of  $S$ .

The formation of the resulting linear system is straightforward but lengthy and will not be reproduced here. It has been directly verified that the equilibrium equation is exactly satisfied and that the boundary conditions are everywhere fulfilled when  $M \rightarrow \infty$ . It was also found that a degree of truncation  $M = 3$  is sufficient to assure a precision of 2.5% for the volume growth rate of the cavities.

## 4. Simulation of porosity evolution

### 4.1 Cavity nucleation

It has been reported [10] that the cavity density on grain boundaries is often proportional to the macroscopic creep strain. More specifically, if  $\dot{\epsilon}$  is the creep strain rate, the cavity nucleation rate for several alloys was found to be

$$\dot{n} = \alpha_p \dot{\epsilon}, \quad (15)$$

where  $\alpha_p$  typically lies in the range  $[10^{10} \text{ m}^{-2}, 4 \times 10^{12} \text{ m}^{-2}]$ . In polycrystalline materials, the local stresses acting on grain boundaries are difficult to estimate and it is thus not easy to derive a relationship for the nucleation rate as function of the local normal stress from eq. (15). However, in order to obtain realistic magnitudes for the nucleation rate  $\dot{\rho}_{nuc}$  with a prescribed far stress  $\sigma_\infty$ , it is convenient to relate  $\dot{\rho}_{nuc}$  to  $\sigma_\infty$  via an effective creep strain  $\epsilon_\infty$ , i.e.

$$\dot{\rho}_{nuc} = \alpha_p \dot{\epsilon}_\infty, \quad (16)$$

where  $\dot{\epsilon}_\infty$  and  $\sigma_\infty$  are related via the Norton law for dislocation creep

$$\dot{\epsilon}_\infty = A \frac{D_v \mu b}{kT} \left( \frac{\sigma_\infty}{\mu} \right)^n, \quad D_v = D_{v0} \exp\left( -\frac{Q_v}{kT} \right). \quad (17)$$

While eq. (15) is an empirical result in which  $\epsilon$  represents the overall creep strain of a polycrystalline specimen, it must be stressed at this level that the creep strain in eq. (16) is rather a scaling value than a real creep strain, since the configuration considered here is that of an unconstrained (or infinite) grain boundary.

Cavities are here assumed to randomly nucleate in time and space according to Poisson spatial and time processes. Through the nucleation process, cavities that overlap other already existing cavities are rejected. The initial cavity size  $a_{init}$  is taken randomly according to one parametric Maxwell distribution with density

$$p(a_{init}) = \sqrt{2/\pi} a_{init}^2 e^{-\frac{a_{init}^2}{2\mu^2}} / \mu^3 \quad \text{and mean value } \bar{a}_{init} = 2\sqrt{2/\pi} \mu.$$

In practice, the number of pores  $\Delta N$  generated during a time interval  $\Delta t$  is random with a Poisson distribution of expectancy  $E(\Delta N) = \pi R^2 \alpha_p \dot{\epsilon} \Delta t$ .

### 4.2 Cavity growth

The growth of  $N$  cavities by grain boundary diffusion is described by the system of  $N$  coupled differential equations (11) for the volume growth rate. In the present work, these equations have been integrated with an explicit scheme.

### 4.3 Coalescence

When two cavities touch, they are assumed to coalesce. Since surface diffusion is throughout assumed to be fast, the new cavity is assumed to immediately reach its equilibrium shape. The total cavity volume is supposed to be conserved during the process: The volume of the new cavity is the sum of the volumes of the old cavities. As a consequence, the cavitated area of the grain boundary decreases.

### 4.4 Sintering

Cavities are allowed to shrink if their growth rate is negative. Below a critical size  $a_{\min} = \bar{a}_{\text{init}} / 10$  the cavities are assumed to disappear.

## 5. Results

### 5.1 Calculation of cavity growth rates

To demonstrate the effect of random cavity spacing, a regular and a random cavity distribution are compared. Numerical values are taken from [19] for copper at 500°C, i.e.  $\Omega = 1.18 \times 10^{-29} \text{ m}^3$ ,  $\gamma_s = 1.78 \text{ J m}^{-2}$ ,  $\delta D_{gb0} = 4 \times 10^{-15} \text{ m}^3 \text{ s}^{-1}$ ,  $Q_b = 1.04 \cdot 10^5 \text{ J/mole}$  and  $\psi = 70^\circ$ . In this section, the cavity size is uniform  $a = a_{\text{init}} = 5 \times 10^{-6} \text{ m}$ , the radius of the RGBE  $R = 8.92 \times 10^{-5} \text{ m}$ , and the normal far stress  $\sigma_\infty = 20 \text{ MPa}$ . The RGBE contains 19 cavities, corresponding to a cavitated area fraction  $\omega = S_d / S_0 = 0.06$ . The distributions of cavities with the isovalue lines of the local normal stress  $\sigma$  can be seen in Fig. 2.

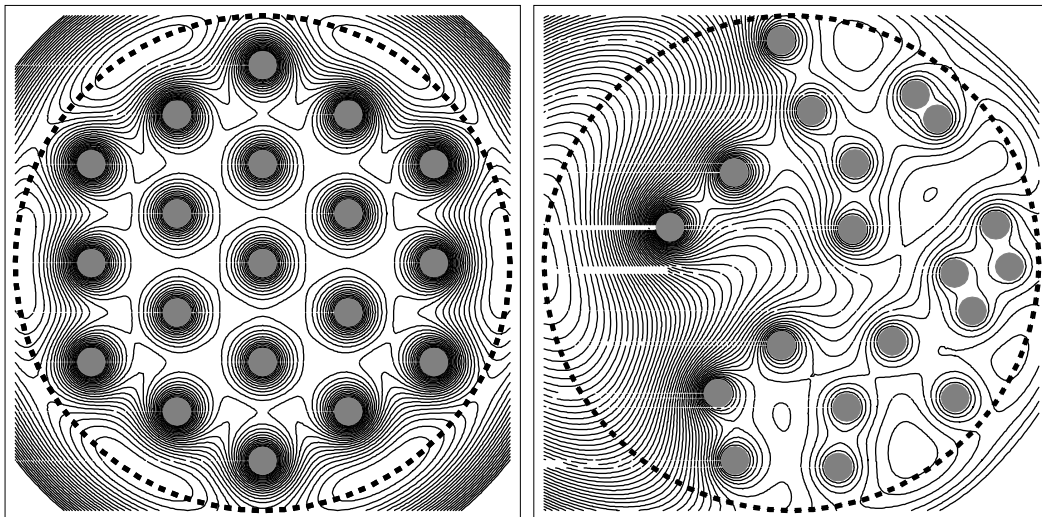


Fig 2a: Isovalue lines of the stress for a regular cavity distribution.

Fig 2b: Isovalue lines of the stress for a random cavity distribution.

For comparison, the distance between the isovalue lines is equal to  $\Delta\sigma = 1.6 \text{ MPa}$  in both cases. The corresponding volume growth rates are compared in Fig.3 with the axisymmetric reference solution (see e.g. [2]) for the volume growth rate

$$\dot{V}_{ref} = 8\pi D \frac{[\sigma_{\infty} - (1-\omega)\sigma_i]}{q(\omega)}, \text{ where } q(x) = -2\ln(x) - (3-x)(1-x) \quad (18)$$

of a single cavity of radius  $a$  in a disk of radius  $c$ , such that the cavitated surface fraction  $\omega = (a/c)^2$  is identical in all cases.

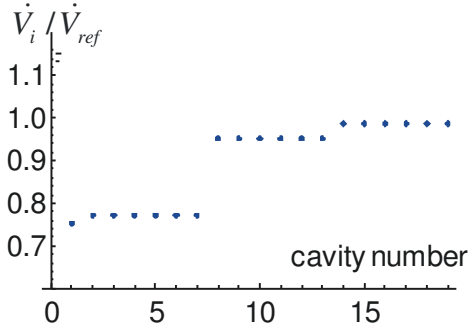


Fig. 3a: Cavity growth rate for a regular arrangement.

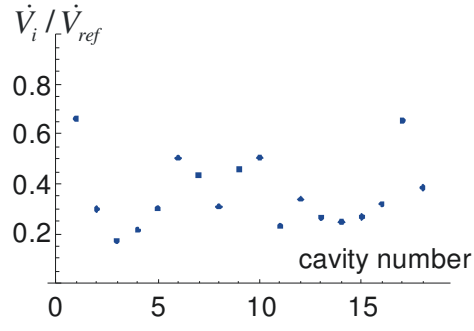


Fig. 3b: Cavity growth rate for a random distribution.

For the regular and the random distributions, the cavity growth rate is lower than the reference solution. The randomness of cavity spacing significantly reduces the calculated growth rates as already found in [7] and [8] for one-dimensional cavity arrays. Indeed, cavity growth is partially constrained by the condition of rigid grains and the existence of zones with low stress gradient, i.e. low diffusive atom flux, or cavity free zones leading to long diffusion paths (see Fig. 2b).

## 5.2 Simulation of porosity growth

The cavitation process has been simulated for two values of the nucleation rate  $\alpha_p = 4 \times 10^{10} \text{ m}^{-2} \text{ s}^{-1}$  and  $\alpha_p = 4 \times 10^{11} \text{ m}^{-2} \text{ s}^{-1}$ ,  $\sigma_{\infty} = 20 \text{ MPa}$  and an average initial cavity size  $\bar{a}_{init} = 2 \times 10^{-6} \text{ m}$ . The numerical constants of the Norton law (17) are taken from ref. [19],  $A = 5.54 \times 10^6$ ,  $D_{v0} = 2 \times 10^{-5} \text{ m}^2 \text{ s}^{-1}$ ,  $Q_v = 1.97 \times 10^5 \text{ J/mol}$ ,  $\mu = 4.2 \times 10^{10} \text{ Pa}$ ,  $b = 2.56 \times 10^{-10} \text{ m}$  and  $n = 5$ . Rupture ( $t = t_R$ ) is assumed to occur at a cavitation fraction  $\omega = 0.5$ . Fig. 4 shows an example of the porosity evolution for the low nucleation rate. At a certain stage, the fraction of small pores decreases due to coalescence events and sintering.

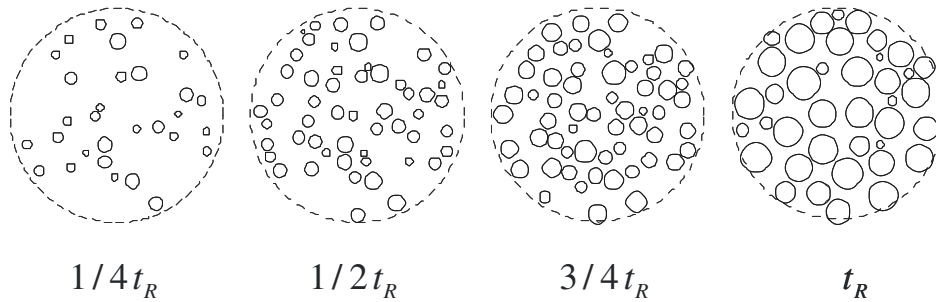


Fig. 4: Evolution of porosity for  $\alpha_p = 4 \times 10^{10} \text{ m}^{-2} \text{ s}^{-1}$ .

Failure occurs at  $\varepsilon = 0.34$  with the low nucleation rate and  $\varepsilon = 0.09$  with the high nucleation rate. The size histograms at rupture normalized by  $\bar{a}_{init}$  are compared in Fig. 5. With the high nucleation rate, the overall process is mostly controlled by nucleation since the amount of cavity growth is rather limited.

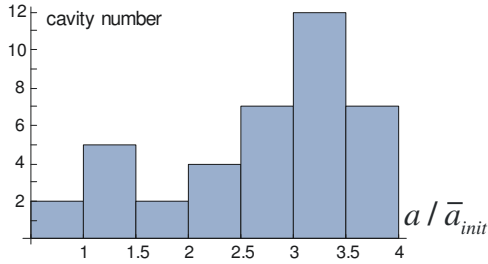


Fig. 5a: Cavity size histogram for  $\alpha_p = 4 \times 10^{10} \text{ m}^{-2} \text{ s}^{-1}$  at rupture.

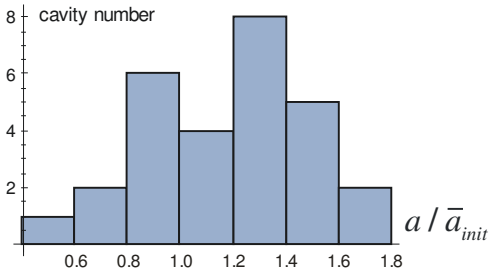


Fig. 5b: Cavity size histogram for  $\alpha_p = 4 \times 10^{11} \text{ m}^{-2} \text{ s}^{-1}$  at rupture.

To assess the impact of heterogeneous size distribution, random spacing and coalescence on the overall damage evolution, we again compare the simulation results with the reference axisymmetric solution (18). To take the reduction of cavity spacing resulting from nucleation into account, the radius  $c$  is now assumed to decrease according to  $\pi c^2 \dot{\rho}_{nuc} = 1$ , where  $\dot{\rho}_{nuc}$  is given by eq. (16). The damage evolutions for both nucleation rates are compared in Fig. 6. In both cases, the homogeneous solution (Reference) overestimates the damage growth rate. This result is fully consistent with the simulations of one-dimensional cavitation reported in [12], [13] and [16].

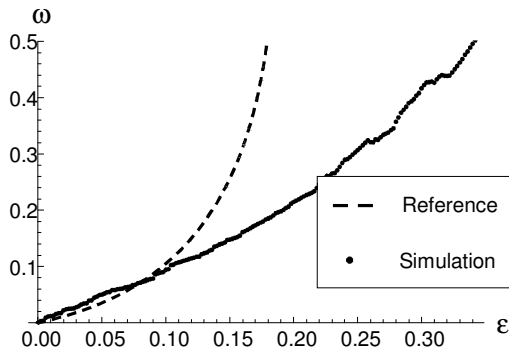


Fig. 6a: Damage evolution for  $\alpha_p = 4 \times 10^{10} \text{ m}^{-2} \text{ s}^{-1}$ .

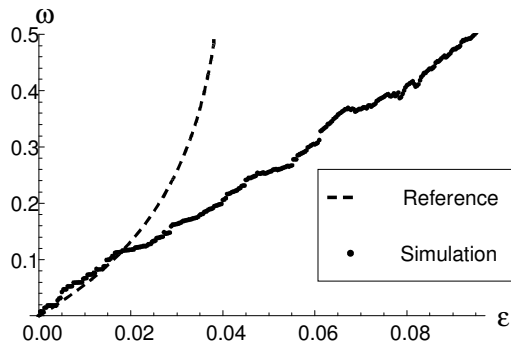


Fig. 6b: Damage evolution for  $\alpha_p = 4 \times 10^{11} \text{ m}^{-2} \text{ s}^{-1}$ .

The Fig. 7a shows that the cavity density decreases after a certain stage, due to sintering and coalescence events. The amount of grain separation (grain boundary

thickening) is calculated as  $\llbracket u^p \rrbracket = \frac{4\pi}{3S_0} \sum_{i=1}^N a_i^3$ , normalized by  $\bar{a}_{init}$  and shown in

Fig. 7b. Again, the homogeneous solution strongly overestimates the grain separation. An evaluation of the pore size distribution is thus required to estimate the amount of grain boundary thickening and hence the degree of constraining of porosity growth.

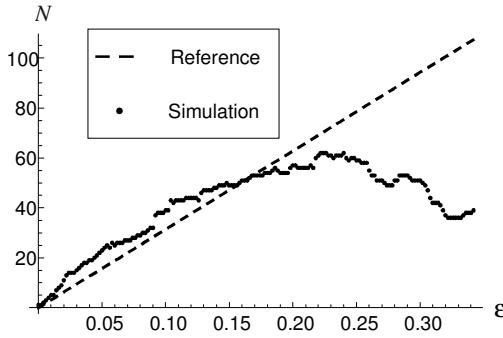


Fig. 7a: Evolution of the cavity number for  $\alpha_p = 4 \times 10^{10} \text{ m}^{-2} \text{ s}^{-1}$ .

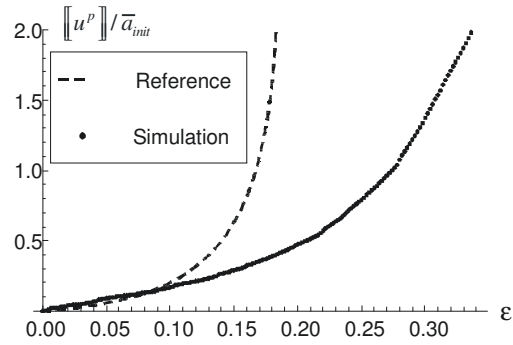


Fig. 7b: Evolution of  $\llbracket u^p \rrbracket$  for  $\alpha_p = 4 \times 10^{10} \text{ m}^{-2} \text{ s}^{-1}$ .

## 6. Conclusions

A new solution to the grain boundary diffusion problem has been integrated in a simulation procedure of creep cavitation. It can be applied in situations in which the contribution of dislocation creep to cavity growth and the effect of cavity surface diffusion can be neglected. The method can be used to identify the relationship between grain boundary thickening and the local acting stresses on the boundary, provided the void nucleation mechanisms are known. By this means, a cohesive law for the grain boundary can be determined and used in a polycrystalline model to estimate stress redistributions during creep.

## 7. Acknowledgements

Financial support by the German Research Foundation (DFG) is gratefully acknowledged.

## 8. References

- [1] D. Hull, D.E. Rimmer, The growth of grain-boundary voids under stress, *Phil. Mag.* 4 (1959) 673-687
- [2] H. Riedel, *Fracture at High Temperatures*, Springer Verlag, Berlin, 1987
- [3] J.R. Rice, Constraints on the diffusive cavitation of isolated grain boundary facets in creeping polycrystals, *Acta Met.* 29 (1981) 675-681
- [4] E. van der Giessen, V. Tvergaard, Development of final creep failure in polycrystalline aggregates, *Acta metall. mater.* 42 (1994) 959-973

- [5] P. Onck, E. van der Giessen, Microstructurally-based modelling of intergranular creep fracture using grain elements, *Mech. Mater.* 26 (1997) 109-126
- [6] S.J. Fariborz, D.G. Harlow, T.J. Delph, The effects of nonperiodic void spacing upon intergranular creep cavitation, *Acta metal.* 33 (1985) 1-9
- [7] J. Yu, J. O. Chung, Creep rupture by diffusive growth of randomly distributed cavities-I. Instantaneous cavity nucleation, *Acta metall. mater.* 38 (1990) 1423-1434
- [8] J.J. Chyou, T.J. Delph, Some effects of random creep cavity placement along a planar grain boundary, *Scripta Met.* 22 (1988) 871-875
- [9] D.S. Wilkinson, The effect of non uniform void distribution on grain boundary void growth during creep, *Acta metal.* 36 (1988) 2055-2063
- [10] B.F. Dyson, Continuous cavity nucleation and creep Fracture, *Scripta Metall.* 17 (1983) 31-37
- [11] A. Ayensu, T. G. Langdon, The inter-relationship between grain boundary sliding and cavitation during creep of polycrystalline copper, *Met. Mat. Trans.* 27A (1996) 901-907
- [12] S.J. Fariborz, D.G. Harlow, T.J. Delph, Intergranular creep cavitation with time-discrete stochastic nucleation, *Acta metal.* 34 (1986) 1433-1441
- [13] J. Yu, J. O. Chung, Creep rupture by diffusive growth of randomly distributed cavities-II. Continuous cavity nucleation, *Acta metall. mater.* 38 (1990) 1435-1443
- [14] D.S. Wilkinson, The effect of time-dependent void density on grain boundary creep fracture-I. Continuous void coalescence, *Acta metall.* 35 (1987) 1251-1259
- [15] D.S. Wilkinson, The effect of time-dependent void density on grain boundary creep fracture-II. Continuous nucleation, *Acta metall.* 35 (1987) 2791-2799
- [16] C. Westwood, J. Pan, A.D. Crocombe, Nucleation, growth and coalescence of multiple cavities at a grain-boundary, *Eur. J. Mech. A/Solids* 23 (2004) 579-597
- [17] S. Axler, Harmonic functions from a complex analysis viewpoint, *The American Mathematical Monthly* 93 (1986) 246-258
- [18] J. Owen, Modélisation de la cavitation des joints de grains sous chargement de fluage, *Ecole Nationale des Ponts et Chaussées, Rapport de stage scientifique (in French)* 2008
- [19] J.S. Wang, L. Martinez, W.D. Nix, A study of intergranular cavity growth controlled by the coupling of diffusion of diffusion and power law creep, *Acta metall.* 31 (1983) 873-881